

NUCLEAR STRUCTURE -- THEORY

THEORY OF LI-11

G. Bertsch and H. Esbensen^a

The nucleus ^{11}Li , on the very edge of the neutron drip line, has attracted much interest recently, having been studied in a number of experiments, eg. refs. 1,2. Its very small binding energy, ~ 200 keV, make it quite unusual. We made a model for the ground state of this nucleus treating it as two neutrons weakly bound to an inert core³. With such a model, one could hope to calculate the binding energy and the low spectroscopy, including electromagnetic matrix elements to continuum states. However, because the single-particle wave functions of such small binding energies extend very far from the nuclear surface, there are technical difficulties in constructing accurate wave functions.

Our approach is to simplify the residual interaction, treating it as a density-dependent delta-function potential. The interaction between the valence neutrons and the core is modelled with a Woods-Saxon potential of such depth as to reproduce the single-particle behavior in ^{10}Li . The strength of the interaction in free space is such as to give a nearly bound state in the free neutron-neutron system. This can be achieved with a delta-function interaction if the space of single particle states is truncated. We chosen a truncation energy of 40 MeV, and the corresponding interaction strength is -830 MeV-fm³. This is a very strong attraction that must be attenuated in the nuclear interior to give sensible results. We chose the density dependence to reproduce the effective pairing interaction in the more tightly bound p-shell nuclei.

We represent the wave function in a single-particle basis, discretized by a box boundary condition at a radius of 40 fm. There are about 2,500 two-particle states, and the eigenfunctions are determined either by matrix diagonalization or a faster Green's function method described in ref. 3. The computed binding energy as a function of the assumed single-particle resonance energy is shown in Fig. 1. The experimental value of the resonance energy is about 800 keV. From Fig. 1, this implies a very weakly bound state, as seen experimentally. The corresponding resonance energy in ^9He is 1.2-1.5 MeV, and no bound state is predicted there. This also agrees with nature.

We have also calculated the dipole excitation strength function within our model. The Coulomb excitation experiments measuring the breakup of ^{11}Li depend on an integral over the dipole strength function, so the model can be directly tested. Our predicted dipole strength function is shown in Fig. 2, compared to a simple single-particle model⁴. We see a very strong concentration of strength at low energy.

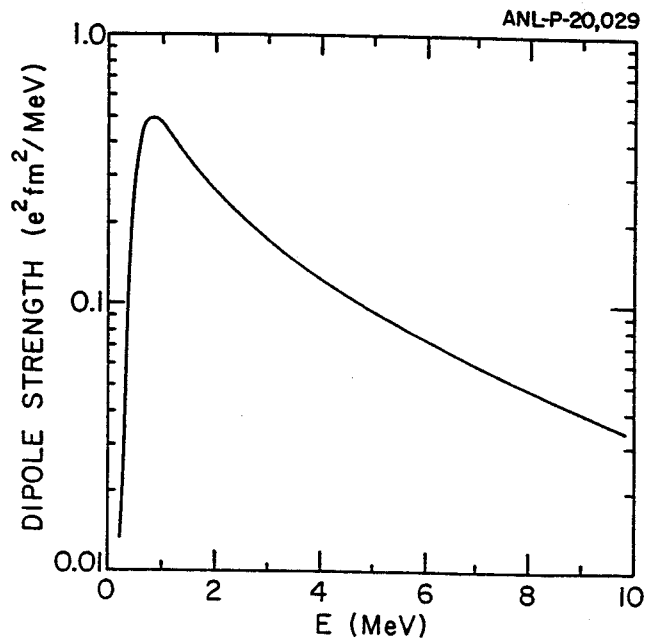


Figure 1: Binding energy of ^{11}Li , shown as a function of the p1/2 resonance energy in ^{10}Li .

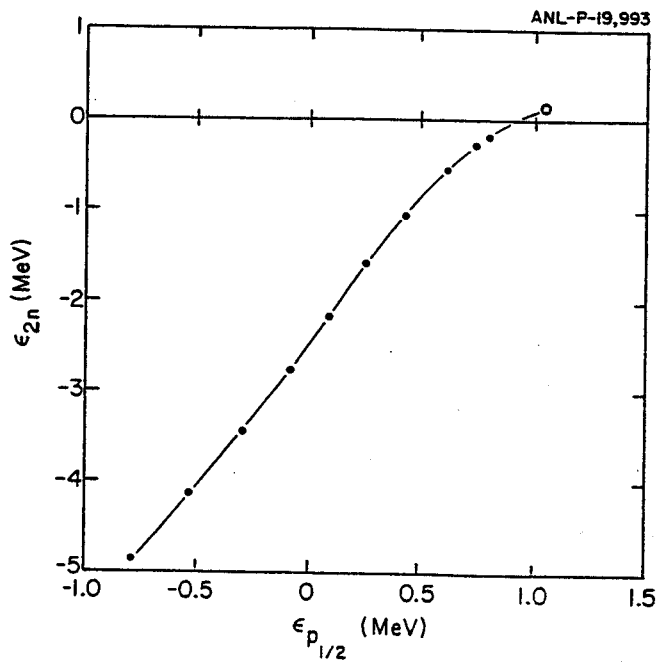


Figure 2: Predicted dipole strength function in ^{11}Li , plotted as a function of excitation energy.

This produces an unusually large Coulomb dissociation cross section. For the conditions of ref. 1, the predicted Coulomb cross section is 570 mb. Experimentally, only the sum of the nuclear and coulomb dissociation is measured. Using an eikonal reaction model⁵, a value of 600 mb was extracted from the experimental measurement¹. However, at lower beam energies the model does not have enough excitation strength⁶. We believe that in the vicinity of the threshold our model underestimates the strength. This is because we have not included the residual interaction in the final state. The attraction between the two neutrons in the continuum states is expected to shift excitation strength downward to even lower energy.

We are presently working on inclusion of the residual interaction in the final state. This would enable us also to make predictions of the correlation between the particles in the final state, which is also feasible to measure.

a. Argonne National Laboratory, Argonne, IL

References

1. T. Kobayashi et al., Phys. Lett. B232 (1989), p 51.
2. R. Anne, et al., Phys. Lett. B250 (1990), p 19.
3. G. Bertsch and H. Esbensen, Ann. Phys. in press.
4. G. Bertsch and J. Foxwell, Phys. Rev. C41 (1990), p 1300.
5. G. Bertsch, H. Esbensen, and A. Sustich, Phys. Rev. C42 (1990), p 758.
6. A. Sustich, to be published.

ENERGY DEPENDENCE OF ^{11}Li DISSOCIATION CROSS SECTION

A. Sustich

The structure of the neutron-rich nucleus ^{11}Li has been the subject of a great amount of recent discussion. The two-neutron separation energy for ^{11}Li is $S_{2n}=0.25\pm.10$ MeV. This very weak binding allows these two valence neutrons to be found at large distances from the more tightly bound ^9Li core, thus forming the neutron halo. Furthermore, ^{10}Li is unbound by $0.80\pm.25$ MeV. Thus, the interaction between the two valence neutrons is as important as the mean field potential for the stability of ^{11}Li . Because of this, one expects a correlation to exist in the wave function of these valence neutrons. To examine the effect of this correlation, one must go beyond a mean field description. Cluster models^{1, 2, 3} which consider a two body problem consisting of ^9Li core plus dineutron and three body models^{4, 5} which treat the $^9\text{Li}+n+n$ system have been proposed.

We calculate the $^9\text{Li}+2n$ breakup cross section due to nuclear interaction by assuming that any removal of the valence neutrons from their initial state will lead to the $^9\text{Li}+2n$ breakup.⁶ For impact parameters less than b_{min} (sum of the ^9Li core radius plus the target radius), the ^9Li core will also interact and result in a more complex breakup than $^9\text{Li}+2n$. The probability of a nucleon remaining in its initial state is

$$P_0(b) = |\langle \psi_0 | e^{i\chi(\vec{b}+\vec{r})} | \psi_0 \rangle|^2 \quad (1)$$

$$= \left| \int d^3r \rho_0(\vec{r}) e^{i\chi(\vec{b}+\vec{r})} \right|^2, \quad (2)$$

where $\rho_0(\vec{r}) = |\psi_0(\vec{r})|^2$ is the density distribution of the nucleon in question and the eikonal phase χ is

$$\chi(\vec{b}) = \frac{-1}{\hbar v} \int_{-\infty}^{\infty} dz V(\vec{b}, z), \quad (3)$$

The cross section is given by

$$\sigma_{-2n}^{nuc} = \int_{b_{min}}^{\infty} 2\pi b db (1 - P_0^2(b)). \quad (4)$$

For the nuclear potential, we use a global fit to neutron scattering data given by Hodgson.⁷ We consider two targets, ^9Be and ^{197}Au . The cross sections obtained are 355 mb for ^9Be and 897 mb for ^{197}Au . The experimental value for a ^9Be target is 470 ± 100 mb. Allowing for about 10 mb due to Coulomb dissociation, we scale our results by 1.30. Our result for ^{197}Au becomes 1.16 b, which together with the experimental cross section of 5.0 ± 0.8 b, gives an extracted Coulomb dissociation cross section of 3.8 ± 0.8 b.

The Coulomb dissociation cross section can be calculated using the formula for dipole excitation probability by a relativistic Coulomb field.^{8,9} At a given impact parameter b with respect to a target of charge Z_2 , this probability is

$$P(b) = \frac{16\pi Z_2^2 e^4 B(E1, \uparrow) \xi^2}{9\hbar^2 v^2 b^2} (K_1^2(\xi) + K_0^2(\xi)/\gamma^2), \quad (5)$$

where the projectile velocity is v and its Lorentz dilation factor is γ . The adiabaticity parameter is

$$\xi = \frac{E}{\hbar\gamma v} \left(b + \frac{\pi Z_1 Z_2 e^2}{2 m_0 v^2 \gamma} \right), \quad (6)$$

where m_0 is the reduced mass of the projectile-target system and E is the transition energy. The dipole transition strength is

$$B(E1, \uparrow) = \frac{1}{(2I_i + 1)} \sum_{f, m_f, m_i, m} |\langle I_f, m_f | M(E1, m) | I_i, m_i \rangle|^2 \quad (7)$$

where

$$M(E1, m) = \frac{N}{A} \sum_p r_p Y_{1,m} - \frac{Z}{A} \sum_n r_n Y_{1,m} \quad (8)$$

is the usual isovector dipole operator. Neglecting any coherence between Coulomb and nuclear amplitudes, the Coulomb dissociation cross section is given by

$$\sigma_{-2n}^{coul} = \int_0^\infty T(b) P(b) 2\pi b db \quad (9)$$

where $T(b)$ is the probability that the projectile is transmitted with no interaction with the nuclear field.

The Coulomb dissociation cross section is determined by the dipole transition strength $B(E1, \uparrow)$. We compare the predicted transition strengths of three different models. The first is a shell model plus RPA calculation.⁵ The second model we investigate uses the correlated ground state of Bertsch and Esbensen⁵ as the initial state. The final model is a cluster model of Bertulani.^{1,2} The dipole strength distribution of the three models is shown in Figure 1.

In Table 1, we show the predictions of the models along with the experimental data for 790 MeV/u ^{11}Li on ^{208}Pb and 30 MeV/u ^{11}Li on ^{197}Au . At the lower energy, the Coulomb contribution is greatly enhanced, which diminishes the problem of subtracting the nuclear contribution.

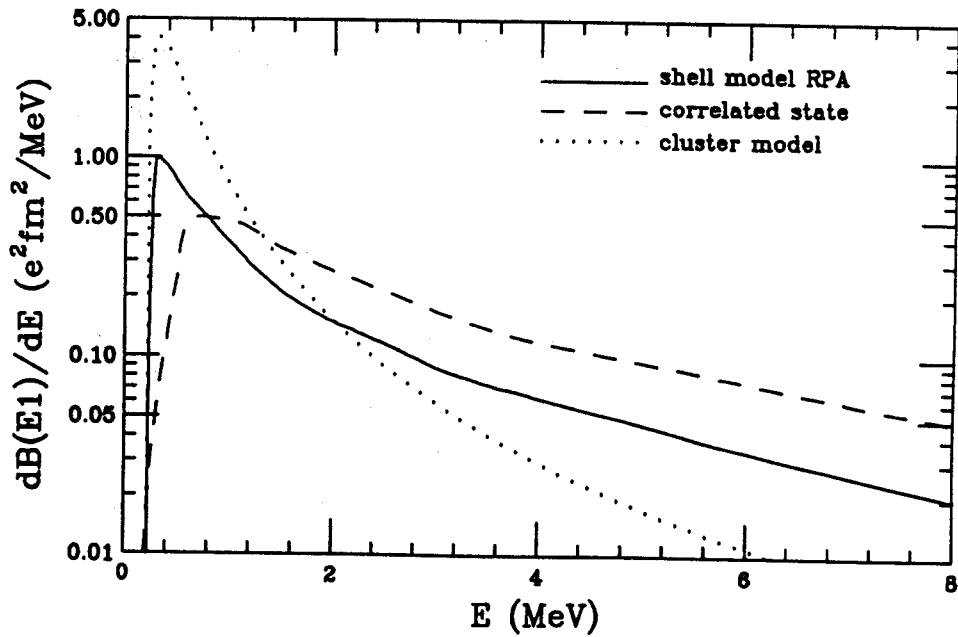


Figure 1. Dipole transition strength distribution given by the three models.

Table 1. Summary of $^{11}\text{Li} \rightarrow ^9\text{Li} + 2n$ breakup cross sections on heavy targets. The experimental data are taken from Ref. 10,11.

		^{208}Pb (E/A=800MeV)	^{197}Au (E/A=30MeV)
$\sigma^{expt.}$		$1.31 \pm .10$ b.	$5.00 \pm .80$ b.
$\sigma^{nucl.}_{model}$		$0.71 \pm .14$	$1.16 \pm .30$
$\sigma^{coul.}_{extracted}$		$0.60 \pm .17$	$3.84 \pm .85$
$\sigma^{coul.}$	shell model RPA	0.508	2.94
	correlated state	0.540	2.02
	cluster model	1.270	8.13

In Figure 2, we show the Coulomb dissociation cross section predicted by the three models as a function of the ^{11}Li bombarding energy on a ^{197}Au target. We have also estimated the cross section for Coulomb excitation of the Giant Dipole Resonance. It is negligible below several hundred MeV/u, but slowly rises until it becomes comparable to the $^9\text{Li} + 2n$ dissociation cross section at energies of 1 GeV/u or higher. While the GDR decay is not expected to contribute very much to the $^9\text{Li} + 2n$ breakup, this is not easily calculated.

At high energies (≥ 500 MeV/u), the predicted cross sections become proportional to the non-energy weighted integrated strength of the models. This is because at these energies the spectrum of equivalent photons¹² seen by the ^{11}Li projectile is almost constant over the energy region where the transition

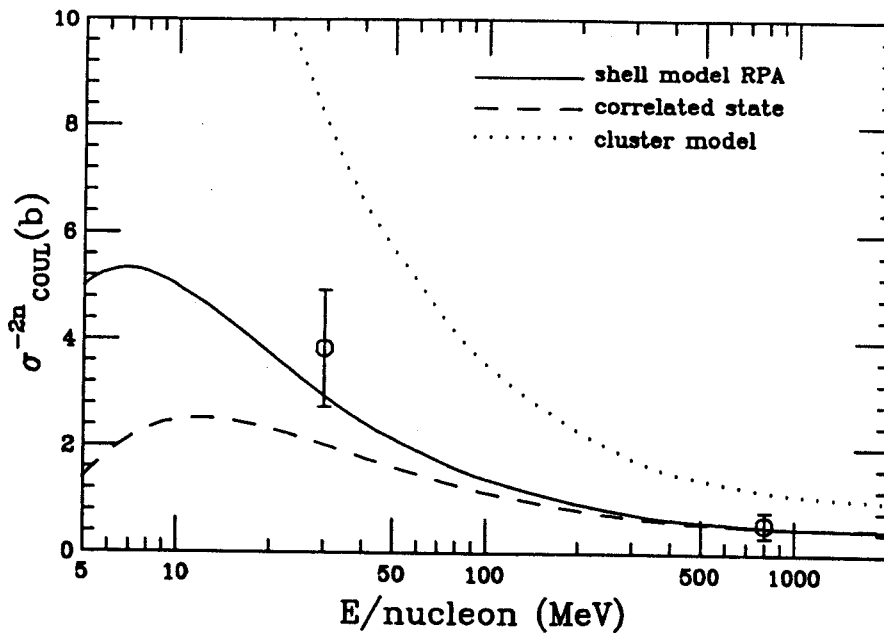


Figure 2. Predicted Coulomb dissociation cross sections for the three models of dipole strength distribution as a function of ^{11}Li bombarding energy for reactions on a ^{197}Au target. The data point at 800 MeV/u is the data for a ^{208}Pb target scaled by $(79/82)^2$. The experimental data are from Ref. 10,11.

strength exists. As the beam energy is decreased, the equivalent photon spectrum develops an exponential dependence and the three models give vastly different predictions due to the difference in how their transition strength is distributed. The cluster model, which has a very large transition strength right at threshold, gives large cross sections at low energy. The correlated initial state model, whose transition strength is distributed more evenly over a broader energy range gives rather small cross sections. The shell model RPA result lies between these two and comes closest to the two data points.

References

1. C.A. Bertulani and M.S. Hussein, Phys. Rev. Lett. **64**, (1990), p 1099.
2. C.A. Bertulani, G. Baur, and M.S. Hussein, Phys. Lett. B, in press.
3. P.G. Hansen and B. Jonson, Europhys. Lett. **4**, (1987), p 409.
4. L. Johannsen, A.S. Jensen, and P.G. Hansen, Phys. Lett. **244B** (1990), p 357.
5. G.F. Bertsch and H. Esbensen, to be published.
6. G.F. Bertsch, H Esbensen, and A. Sustich, Phys. Rev. **C42** (1990), p 758.
7. P.E. Hodgson, Rep. Prog. Phys. **47**, (1984), p 613.
8. A. Winther and K. Alder, Nucl. Phys. **A319**, (1979), p 518.
9. G.F. Bertsch and J. Foxwell, Phys. Rev. **C41**, (1990), p 1300.
10. T. Kobayashi, *et al.*, Phys. Lett. **232B**, (1989), p 51.
11. R. Anne *et. al.*, Nucl. Phys. A, in press.
12. C.A. Bertulani and G. Baur, Phys. Rep. **163**, (1988), p 299.

DIFFUSION COEFFICIENT FOR NUCLEAR SHAPE CHANGES

B. Bush^a and G. Bertsch

It seems apparent from fission experiments that the time scale for shape changes in nuclei is longer than for other processes such as the statistical evaporation of neutrons¹. This time scale is also important in determining the shape of the cross-section and the possibility of nonadiabatic effects in giant dipole resonances of highly excited nuclei^{2,3}. We have constructed a simple microscopic model to determine the time dependence of shape changes and are presently performing numerical calculations for nuclei with $A \approx 80$.

Our approach is quite different from previous theoretical work⁴ in that we focus on individual mean-field configurations and study how they mix via the two-body interaction. When the level density is high enough, the effects of the interaction can be incorporated into rate equations with coefficients evaluated by Fermi's Golden Rule. In the limit of a large number of levels, we can represent the dynamics by a diffusion equation for the shape distribution $P(Q, t)$:

$$\frac{\partial P(Q, t)}{\partial t} = -\kappa(Q) \frac{\partial^2 P}{\partial Q^2}. \quad (1)$$

We have specialized here to quadrupole shape changes, with $Q \propto \sum(2z^2 - x^2 - y^2)$ being the mass quadrupole moment. The diffusion parameter κ is determined in our model by the formula

$$\kappa(Q) = \frac{1}{N_i} \sum_{i,j} \langle i|V|j \rangle^2 \delta(E_j - E). \quad (2)$$

Here i and j label many-particle configurations, and the sum over i ranges over configurations that have deformations close to Q . The j sum includes all configurations connected to i by the residual interaction.

The first question that arises in this formulation is whether the level densities are high enough that the averaging in eq. 2 is sensible. We have investigated this numerically and it seems that the level density is high enough for this purpose for heavy nuclei when the temperature is over 2 MeV. We have also developed an efficient method for evaluating the matrix elements in eq. 2 and are proceeding with the calculation of the diffusion coefficient κ for ⁷⁶Ge. Later we will calculate κ for time nuclei and see whether these theoretical values are consistent with parameters extracted from the shapes of the giant dipole resonance at high excitation energy³.

a. Los Alamos National Laboratory, Los Alamos, NM

References

1. P. Grange, S. Hassani, H. A. Weidenmueller, A. Gavron, J. R. Nix, and A. J. Sierk, Phys. Rev. C34 (1986), p 209.
2. R. A. Broglia, T. Dossing, B. Lauritzen, and B. R. Mottelson, Phys. Rev. Lett. 58 (1987), p 326.
3. Y. Alhassid and B. Bush, Nucl. Phys. A514 (1990), p 434.
4. M. C. Nemes and H. A. Weidenmueller, Phys. Rev. C24 (1981), p 450.

COLLECTIVE MOTION IN DEFORMED NUCLEI

G. Bertsch and H. Flocard^a

Recently, the Orsay-Livermore group studied collective motion in deformed Hg isotopes using Hartree-Fock theory and the generator coordinate model^{1,2}. A possible simplified treatment of collective motion was proposed earlier^{3,4}, called the hopping model. In this work we examine how well the hopping model works in comparison to the more elaborate generator coordinate calculations.

The hopping model is constructed from a discrete basis of states, representing roughly the Hartree-Fock configurations of interest. The number of discrete states is chosen equal to the number of Hartree-Fock level crossings within the deformation range of interest. The diagonal energies of the states are assigned by discretizing the Hartree-Fock-Bogoliubov potential energy surface according to the number of states represented. There is one remaining parameter in the hopping model, the off-diagonal matrix element connecting different states in the discrete basis. It was argued that the only important matrix elements are the ones connecting adjacent states, and that the average size of the matrix element is related to the pairing strength G , and the proton and neutron pairing gaps Δ_n and Δ_p by the formula³

$$v = \frac{\Delta_n^2 + \Delta_p^2}{4G}.$$

The global systematics of pairing⁵ yield values of v in the range 2.5 - 3.0 MeV.

We show first how well the hopping model works for the energy spectrum of ¹⁹⁴Hg. Fig. 1 shows, as the solid curve, the potential energy surface from ref. 2. The solid lines marked with a dot are the eigenstates from the generator coordinate calculation. To construct the hopping model, we next counted the number of level crossings for the deformation range -30 bn to +60 bn in the Hartree-Fock theory, finding 23. Thus the discrete model consists of 23 states, with diagonal energies following the solid line in Fig. 1. The eigenstates are found by diagonalizing the 23 by 23 tridiagonal matrix whose off-diagonal elements are all v . The result, taking $v = 2.5$ MeV, is shown by the dashed lines marked with x in Fig. 1. An overall shift of energy has been added to match the lowest state of the generator coordinate method. We see remarkably good agreement between the two, going up to excitation energies of the order of 8 MeV. There is an isolated superdeformed state in both treatments, and the level spacing is quite reasonable.

We next examine some properties associated with the wave function. The ground state wave function for ¹⁹⁴Hg is shown in Fig. 2. The smooth curve is the result of the generator coordinate method,

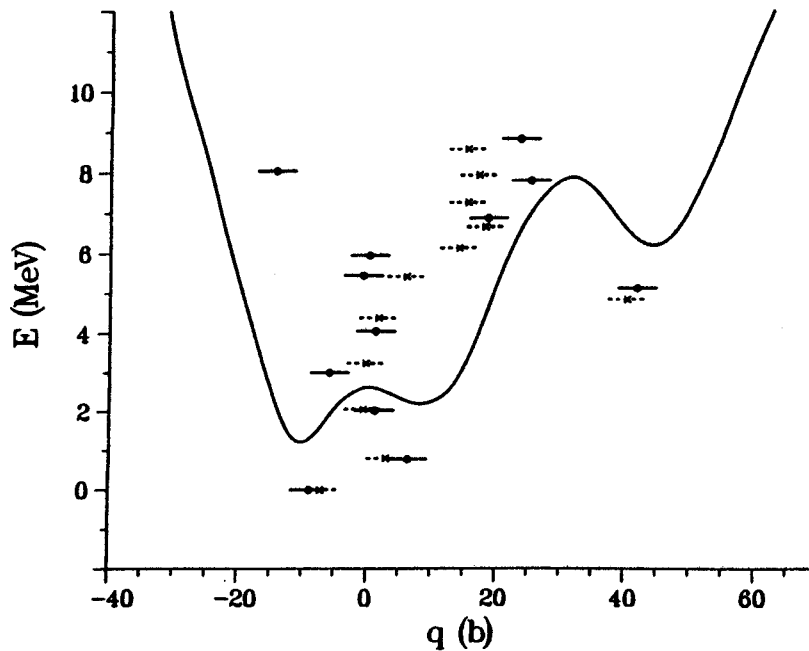


Figure 1: Energy as a function of deformation in ^{194}Hg .

and the histogram is the corresponding wave function in the discrete-basis hopping model. We see that the agreement is quite close.

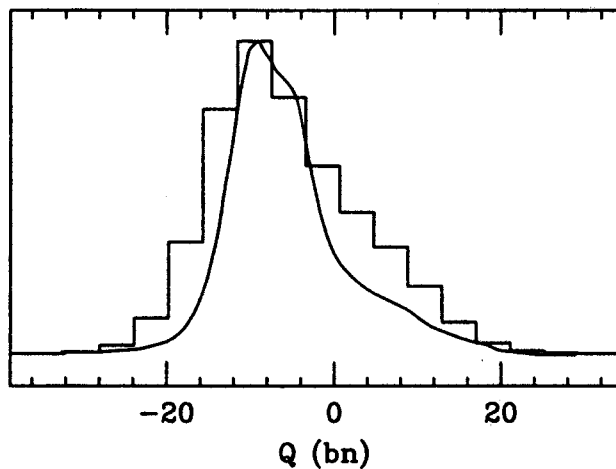


Figure 2: Ground state wavefunction in ^{194}Hg .

An important physical quantity is the quadrupole matrix element between different eigenstates. This will indicate, for example, whether a superdeformed state can decay by a quadrupole transition to the ground state band, or whether it is so hindered in this process that it would decay by statistical E1 transitions instead. In ref. 2 the matrix elements were quoted for ^{190}Hg and ^{198}Hg . We show these results

in Table 1, compared with the corresponding result of the hopping model. The results agree very well. The conclusion would be that in the lighter isotope a collective E2 transition out of the superdeformed band is possible, but that it is unlikely to dominate in the heavier nucleus.

	GCM	Hopping Model
^{190}Hg	1/300	1/150
^{198}Hg	10^{-4}	10^{-4}

Table 1: Off-Diagonal quadrupole matrix elements. The quadrupole matrix element between the superdeformed state and the ground state, divided by the expectation value in the superdeformed state, is compared. The first column is from the wave function in the generator coordinate calculation, ref. 1. The second column is the hopping model discussed in the text.

We regard these results as extremely encouraging to simplified modelling the collective shape dynamics. It is rather easy to find potential energy surfaces in the literature. The counting of level crossings is however less accessible. We would urge authors who publish potential energy surfaces to also show their single-particle energies, from which the level crossing information can be obtained.

a. IPN, Orsay

References

1. P. Bonche, et al., Nuclear Physics A510 (1990), p 466.
2. P. Bonche, et al., Nucl. Physics A, to be published.
3. G. Bertsch, in Proceedings of the International School of Physics, Enrico Fermi CIV, (So. Italiana di Fisica, Bologna, 1988), p. 41.
4. F. Barranco, et al., Nuclear Physics A512 (1990), p 253.
5. A. Bohr and B. Mottelson, Nuclear Structure (Benjamin, N.Y., 1969,1975), Eq. I-2-94 and II-6-591.

DECAY OF SUPERDEFORMED NUCLEI

G. Bertsch and D.M. Brink^a

Superdeformed bands are commonly observed to decay into the normal states over 2-4 transitions within the superdeformed band. This poses the question for theorists of how well the decay can be calculated, and whether it provides information on such issues as large-amplitude collective motion. In this work, we examined a mechanism for the decay which treats it as a two-step process^{1, 2, 3, 4}. There is first a probability p_i that the superdeformed state mixes with an ordinary state i . Then, the two kinds of states decay with widths Γ_Q and Γ_c , respectively. With these assumptions the total probability to decay out of the band is⁴

$$P_{out}(I) = \sum_i \frac{p_i(1-p_i)\Gamma_c}{p_i\Gamma_Q + (1-p_i)\Gamma_c}. \quad (1)$$

There is a simple approximate expression for P_{out} in the weak coupling limit when $p_0 \approx 1$ and $(1-p_0) \ll 1$. Writing $P_{in} = 1 - P_{out}$ we have

$$P_{out}/P_{in} \approx (1-p_0) \frac{(\Gamma_c + \Gamma_Q)}{\Gamma_Q}. \quad (2)$$

Thus there can be strong transitions out of a superdeformed band even in the weak coupling limit provided Γ_c/Γ_Q is large enough. Another simple limit corresponding to a moderate coupling situation is obtained by assuming that the superdeformed strength is uniformly spread over n states. Then

$$P_{out}/P_{in} = n\Gamma_c/\Gamma_Q. \quad (3)$$

The limits (2) and (3) give a qualitative idea about the way in which the transition probability out of a superdeformed band depends on the coupling strength and on the ratio Γ_c/Γ_Q .

To examine the dependence of the branching ratio on the parameters in more detail, we applied eq. (1) to a simple numerical model. A superdeformed state was coupled to a set of 20 normal states with a constant coupling matrix element V . The normal states were taken to have equal spacing D and the unperturbed superdeformed state was separated by $D/4$ and $3D/4$ from the two central normal states. The hamiltonian was diagonalized and the transition probability out of the band calculated from eq. (1). We next estimate the parameter values and how they change with each transition. We discuss mainly ¹⁵²Dy, the first discovered example of superdeformation⁵, which also happens to show a rather abrupt decay out

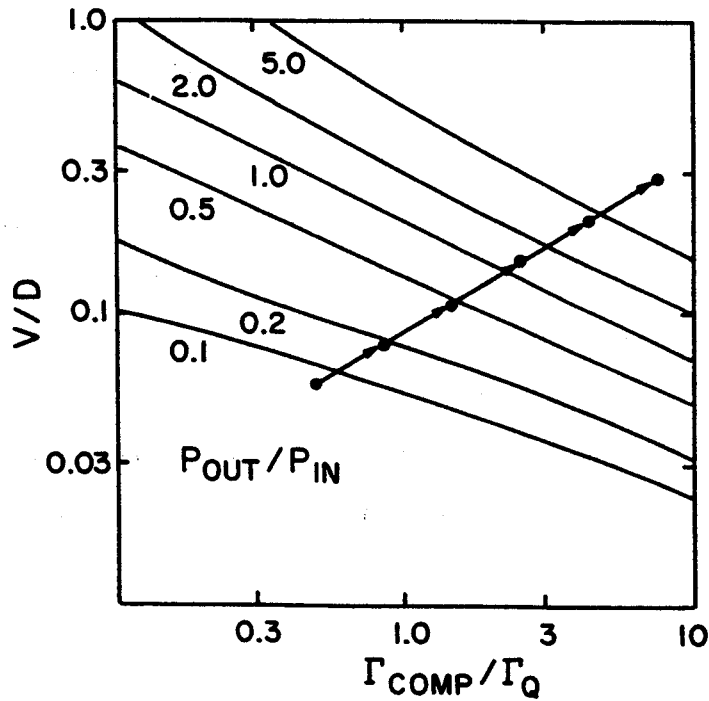


Figure 1: The branching ratio P_{out}/P_{in} depopulating the superdeformed band as a function of the band mixing parameter V/D and the decay width ratio Γ_c/Γ_Q . The chain of arrows shows the sequence of transitions for a hypothetical nucleus similar to ^{152}Dy .

of the band. In ^{152}Dy , the last observed transition is thought to be due to the decay of the $I = 24$ state, and the excitation energy of the band above the yrast line is estimated to be $E^* \approx 4$ MeV at the exit point. The in-band width Γ_Q is known fairly well because the lifetime of states in the band can be measured⁶. For the $I = 24$ decay, the in-band transition energy is 602 keV and $\Gamma_Q = 8$ meV.

We now consider the decay width Γ_c for normally deformed states at the excitation energy of the exit point. The dominant decay mode at $E^* \approx 4$ MeV is probably $E1$. The total gamma widths of compound nucleus states at neutron threshold, $E^* \approx 8$ MeV, have been measured in the Dy region. They are all about 100 meV without much fluctuation. Values at lower excitation energy can be estimated by using the procedures described in ref. 7. The results are very sensitive to the availability of final states with the correct spin and parity and therefore depend on assumptions made about the density of final states. A prescription $\Gamma_c \sim E^{*2}$ which is a simplification of one of the forms used in ref. 7 gives $\Gamma_c \approx 25$ meV for $E^* = 4$ MeV. Using this estimate we find $\Gamma_c/\Gamma_Q \approx 3$. However, this ratio could be reduced by a factor of 2 or 3 if pairing effects are still important for the density of odd-parity states with $I \approx 24$ and $E^* \leq 4$ MeV.

The level spacing D is much more uncertain. For an orientation, we estimate it using a simplified formula⁸ for the density of levels of given spin in an even-even compound nucleus,

$$\rho(E^*, I) = \frac{B(2I + 1)}{(E^* - 2\Delta)^2} \exp(2\sqrt{a(E^* - 2\Delta)}).$$

Here a is the level density parameter, E^* is the excitation energy above the yrast state and Δ is the pairing gap. We choose $a = A/8 \text{ MeV}^{-1}$, $\Delta = 12/\sqrt{A} \text{ MeV}$ and fit B to the spacing of neutron resonances in a nearby nucleus, ^{150}Sm . This yields $D \approx 500 \text{ eV}$. Åberg⁹ has pointed out that the factor $(2I + 1)$ overestimates the spin dependence of the density of states for large I . Thus D should be increased by a factor of about 5 for $I = 24$. If pairing has disappeared for these spin values then there could be a decrease in D by a factor of 40. Clearly, we cannot expect to extract any physics from the decay measurement that requires knowledge of D .

Even though there are considerable uncertainties in Γ_c and D the changes in these quantities with E^* and I are quite well determined if pairing and spin dependence are assumed to change slowly with I . Because of the different moment of inertia of the superdeformed band, we expect E^* to increase by about 300 keV when I changes from 24 to 22. Then Γ_c and D are expected to change by factors of about 1.16 and 0.54, respectively, from one transition to the next. We may safely assume that the intrinsic quadrupole moment of the superdeformed band is constant over the range of interest, which implies that Γ_Q is proportional to E^5 and will be reduced by a factor of 0.68 for the next transition in the band.

Finally, we assume as a hypothesis that the damping width of the superdeformed state into the normal states, $\Gamma^\downarrow = 2\pi V^2/D$, is independent of I over the range of interest, so that $V \sim \sqrt{D}$. Then with each transition V/D and Γ_c/Γ_Q will increase as estimated above, except for statistical fluctuations. The change in branching ratio from one transition to the next is illustrated by the sequence of points connected by arrows in Fig. 1.

We see that the theoretical branching ratios increase by a roughly a factor of 2 with each transition. The experimental branching ratio in ^{152}Dy changes much more rapidly. The two are compared in Fig. 2. Thus we would conclude, in agreement with ref. 3, that there appears to be additional physics requiring Γ^\downarrow to change rapidly with I . However, in other bands found since then the decay out of the band is more gradual. In ref. 4, it was concluded that the ensemble of data is consistent with a purely statistical decay. Certainly, the statistical fluctuations can be large, especially when the parameter V/D is small. There is also a collective mechanism for decay out of superdeformed bands⁷. Quantum collective motion, described by microscopic theories such as the generator coordinate method, causes a mixing of the superdeformed

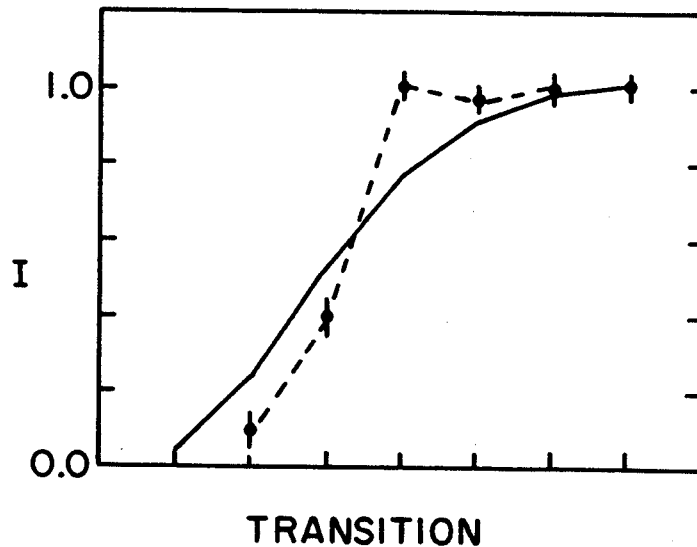


Figure 2: In-band intensities of superdeformed transitions, following the the branching ratios of the hypothetical decay sequence of Fig. 1, are shown by the dashed line. This is compared with the experimental intensities found in ^{152}Dy : (ref. 5).

and normally deformed states. It is then possible to make a quadrupole transition from a superdeformed to a normal state¹⁰. It is interesting to note that in the decays of fission isomers, which represent the first examples of transitions from superdeformed to normal states, both $E1$ and $E2$ decay modes are found¹¹. In any case, the factor of E^5 in the quadrupole decay rate would favor direct decays to the lowest collective band. If this were the main decay mode in the rare earth nuclei, one should expect to see the intermediate gamma transition between the two bands.

a. Dept. of Theoretical Physics, University of Oxford

References

1. Ragnarsson and S. Åberg, Phys. Lett. **B180**, (1986),p 191.
2. B. Herskind, et al., Phys. Rev. Lett. **59** (1987),p 2416.
3. K. Schiffer, B. Herskind and J. Gascon, Z. Phys. **A332** (1989),p 17.
4. E. Vigezzi, R. Broglia and T. Døssing, Phys. Lett. **249** (1990),p 163.
5. P. Twin, et al., Phys. Rev. Lett. **57** (1986),p 811.
6. M.A. Bentley, et al., Phys. Rev. Lett. **59** (1987),p 2141.
7. S. Bjørnholm and J.E. Lynn, Rev. Mod. Phys. **52** (1980),p 851 .
8. A. Bohr and B. Mottelson, Nuclear Structure (Benjamin, 1969), Vol I, eq. (2B-62).
9. S. Åberg, Nucl. Phys. **A477** (1988),p 18.
10. P. Bonche, J. Dobaczewski, H. Flocard, P. Heenen, S. Krieger, J. Meyer, and M. Weiss, Nucl. Phys., to be published.
11. D. Habs, Nucl. Phys. **A502** (1989),p 105.